

PRODUCTION OF A SINGLE COATED GLOSSY INKJET PAPER USING CONVENTIONAL COATING AND CALENDERING METHODS

Hyun-Kook Lee, Margaret K. Joyce,
Paul D. Fleming, and John H. Cameron
Western Michigan University
Department of Paper and Imaging Science and Engineering
Kalamazoo, Michigan 49008

ABSTRACT

The unique structure of precipitated and gelled silicas provides an internal and packing porosity that enables the rapid diffusion of liquid inks into the coating layer. The rapid uptake of the ink immobilizes the anionic dyes at the surface of the coating, allowing high optical print densities to be achieved. However, precipitated and gelled silicas are primarily used in matte grades since the particle size of them is typically 3-16 μm range.

This study focused on the use of non-porous fumed silicas and alumina in glossy inkjet media. The coating process was a single coat blade application on a cylindrical lab coater (CLC) at speeds up to 920 m/min. The use of fumed alumina enabled gloss values of almost 70% to be achieved after 3 passes through a sheet fed soft nip calender at 60 °C and 123 kN/m. The work is significant because it demonstrates the ability to produce glossy inkjet coated papers by applying a single pigmented coating layer on a blade coater and finishing with a soft nip calender. The research described herein examines the contribution of coating structure influences on inkjet print quality. The pigments used are commercially available and are currently being employed in this application.

INTRODUCTION

The quality of non-impact printing is improving as a consequence of increased resolution and the adoption of color printers in the home and office. These trends are placing increasingly stringent requirements on the paper coating. To date, research in the area of paper coatings for inkjet printing has concentrated on examining the paper properties required for good print quality (1). The results of these studies have shown that good print quality depends very much on the structure and the surface properties of the paper coating.

To understand some of the demands placed on a coating during this printing process, a basic understanding of some of the typical ranges of ink and print properties is required. For a typical narrow-format, home/office ink-jet printer, the ink fluid contains 2-5 wt. % colorant (dye or pigment), 2-5 % surfactants and additives, 30 % humectant (ethylene glycol or diethanolamine), and 65% water. The important ink-fluid parameters that contribute to the quality of the printed image are surface tension and viscosity (2).

For current generation printers, the effective resolution of the image (dots per inch or centimeter) is controlled by the dot size; for a 360 dpi image, an individual dot should be approximately 100 microns in diameter, and for a 720 dpi image, the dot size should be approximately 50 microns. For these printers, the droplet volume varies from 150 pL (picoliters) to 40 pL. Since the diameter of liquid spheres of these volumes is considerably smaller than the respective diameters of the dots, it is clear that considerable radial spreading of the droplet typically occurs on the substrate immediately after droplet impact. The dependence of droplet spreading on ink properties (surface tension) as well as coating properties (surface tension, roughness, and porosity) is therefore very important to understand.

Ideally, the dot should be perfectly circular with a fixed diameter; this requires controlled gain, or spreading, of the ink droplet on impact. A typical coating thickness for matte-home/office media is roughly 20 microns. The volume of a cylinder of liquid that measures 60 microns in diameter and 20 microns in length is 56 pL. Since the droplet is 40 pL, the coating void fraction can be taken to be 0.6. Therefore, even one droplet can be considered to saturate this cylindrical volume fraction. Thus, it is clear that for full gamut color printing, which requires the juxtaposition of two or three droplets, the ability of the coating to handle the ink liquids and channel them away from the printing

surface is essential. Furthermore, it is desirable for the colorants to be deposited on or near the surface, as penetration into the base sheet will lower print optical density.

The effect of coating properties on print quality has been shown to depend on the micro- and macro-porosity of the coating (3). Due to the large volume of water contained in the ink, it has been found that a coating capable of quickly absorbing and holding water, to set the ink quickly, is required for good print quality. Penetration of water into the substrate results in fiber swelling which distorts the image, thus reducing the print quality. Undesirable cockling of the sheet can also occur. For these reasons, conventional coatings are largely inadequate for use in color ink-jet printing papers.

The coating media from conventional pigments such as kaolin, calcium carbonate, and titanium dioxide are not widely used for inkjet papers, primarily because of their available void fraction for liquid uptake as well as the narrow pore diameters for fluid flow (0.02 to 0.04 μm). Conventional pigments also require calendering to obtain their gloss and smoothness properties, which reduces the available void fraction for liquid uptake. So, for glossy inkjet papers, a dilemma exists as to how to simultaneously obtain gloss and maintain sufficient void fraction. Coating technologies using silica pigment and polyvinyl alcohol (PVOH) were developed to enable more void volume for liquid uptake. However, precipitated and gelled silica pigments are matte pigments, so they are not suitable for glossy inkjet grades.

Inkjet printing places demands on paper that are quite different from those required by conventional contact printing methods (4). Most inkjet printers require low viscosity and low solids ink to achieve proper jetting. Thus, to obtain images with sufficient optical densities, relatively large volumes of these inks are required. High liquid loading presents a peculiar problem to the design of an optimum inkjet coated paper.

Inkjet Paper Classifications

Inkjet papers can be classified into four major categories as shown in Table 1. Depending on the grade, the coating formulation, and application process (air knife, pre-metering size press, rod, or blade), cost can vary substantially (5,6).

Table 1. The Classification of the Media

Plain or surface-sized paper	Lowest cost, good monochrome text, poor color (limited coverage, poor gamut, high bleed, strike-through, cockle/curl)
Coated matte paper	High cost, good color gamut, fast dry time, excellent resolution, 100% coverage
Coated glossy paper	Higher cost, non-porous, slow dry time, poor waterfastness, slow dry, photorealistic image
Cast coated paper	Highest cost, highest gloss, photorealistic image, multiple coating layers, good water fastness

Glossy inkjet papers are by far the best papers to use when photorealistic images are desired, better even than electrophotographic (laser). They best replicate silver halide photographs (6). They are currently made by one of three processes. One uses a double or triple coat process. Another coats a dense layer composed of a hydrophilic resin onto a plastic film or laminated paper (see Figure 1). This is called a resin-coated paper.

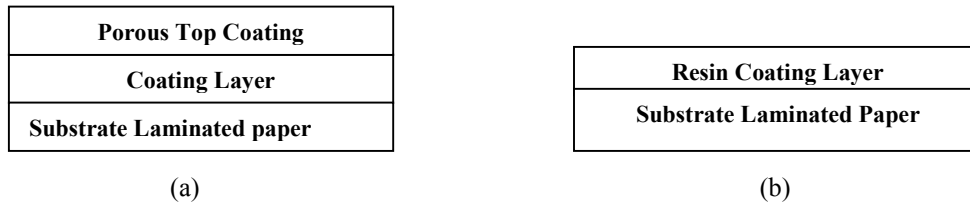
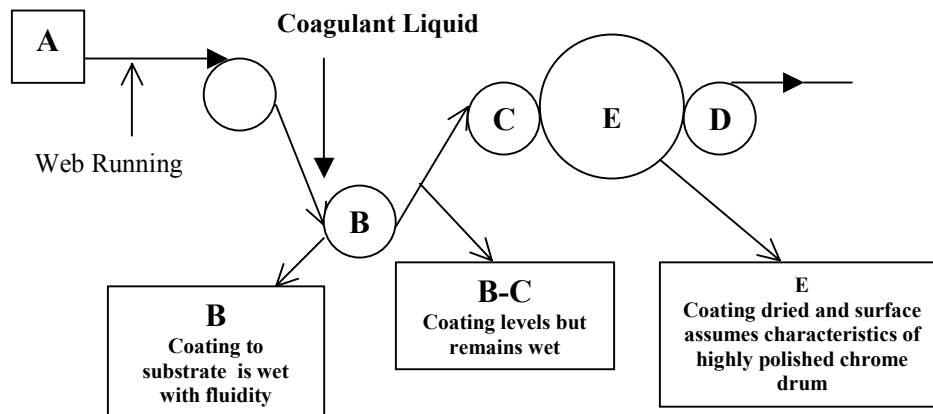


Figure 1. (a) Cross section multicoated paper, and (b) film-substrate glossy based paper.

The third process uses a cast coater to apply a special coating that produces a porous coating layer on a pre-coated paper substrate (7,8). The process for making cast coated papers is shown in Figure 2. The coagulation-method (cast) is specifically suitable for production of glossy inkjet papers due to the replication of the chrome cylinder. It is a highly specialized coater, limited in speed.



A: Coating Operation Part, B: Coagulant Roll, C: Forming Roll, D: Strip Off Roll, E: Heated Metal Drum with Specular Surface called “Cast Drum”

Figure 2. Schematic of the cast-coating Process (adapted from reference 7)

OBJECTIVES

In this study, two fumed silicas and one fumed alumina were used in the preparation of inkjet coating formulations. It was of special interest to determine if the use of the fumed silicas and alumina could provide the desired gloss and void fraction for liquid uptake required of high quality glossy inkjet papers. An understanding of the contribution of coating properties on coating gloss and print quality was sought.

The objectives of this research were:

(A) To study the influence of fumed silica and alumina on the optical properties and printing qualities of coated paper,

(B) To compare the print quality between the fumed pigment coating samples and commercial coated inkjet samples, and

(C) To study the surface properties of the coating using SEM (scanning electron microscopy), dynamic contact angle measurements, and the porous structure of the coating using mercury porosimetry between the fumed pigment coating samples and commercial samples.

EXPERIMENTAL DESIGN

Coating formulations were prepared from two fumed silicas of varying surface areas and one fumed alumina. The physical properties of the pigments used are shown in Table 2.

Table 2. Physical Properties of Pigments as Supplied

Sample	Solids Content %	Color	Specific Gravity (g/cm ³ , 25° C)	Surface Area (m ² /g)	Mean Particle Size (µm)	pH
Fumed Alumina (FA)	40%	White	1.40	55	0.16	3.8-4.2
Fumed Silica A (FSA)	30%	White	1.20	90	0.225	10.0-10.3
Fumed Silica B (FSB)	25%	White	1.20	170	0.145	9.0-10.0

The binder used in the coating formulation was a partially hydrolyzed, low viscosity polyvinyl alcohol (PVOH). This polyvinyl alcohol was chosen to optimize the coatings solids by minimizing the interaction between pigments and PVOH. Polyvinyl alcohols with a higher degree of hydrolysis are known to interact more strongly with silica pigments, thus limiting the coating solids content that can be obtained. The solution of PVOH was prepared at 32-33% solids by adding the required amount of dry PVOH powder to cold water under agitation and heating the mixture to 85 °C. The solution was held at this temperature for 35 - 40 minutes to assure complete dissolution and hydration of PVOH. A defoamer was then added. The solids content of the solution was measured using a CEM Labwave 9000 microwave moisture analyzer.

The PVOH solution was cooled to 25°C before addition to the slurried fumed pigments at a pigment to binder ratio of 4:1 (pigment: 100 parts and binder: 25 parts) under slow agitation. A pigment to binder ratio of 4:1 was selected based upon an extensive study, which showed this ratio to provide the near optimum gloss. The coatings were mixed for 20 - 30 minutes and the pH and viscosity were measured. The viscosities of the coatings were measured using a Brookfield RVT digital viscometer (#5 spindle @ 100 rpm, 25 °C).

The initial low pH (4.4) of the alumina coating formulation was increased with 0.1% KOH to raise the viscosity of the coating without the addition of a thickener. This was necessary to enable the desired coat weights to be achieved on the CLC coater. Table 3 shows the coating properties of each formulation as applied.

Table 3. Properties of Coating Formulations

Coating	Viscosity (cP)	pH	Solid Content (%)
FA + PVOH	1288	8.82	27.18
FSA + PVOH	536	9.26	31.75
FSB +PVOH	536	9.25	27.00

The 75 g/m² wood-free base paper was blade coated using a Cylindrical Laboratory Coater (CLC) at a speed of 610 m/min. Four different coat weights were applied: 6 ± 1 g/m², 9 ± 1 g/m², 12 ± 1 g/m², and 16 ± 1 g/m². The CLC samples were calendered through 3 nips at 123 kN/m and 60°C using a sheet fed hot-soft nip calender.

Additional CLC runs were performed to assess the runnability of the coatings at higher speeds. The fumed alumina coating could be uniformly applied at speeds up to 920 m/min. However, the coating of the fumed silica (B) was limited to 610 m/min, because above this speed, undesirable streaks and spits were found and coat weight uniformity suffered.

The brightness, gloss, smoothness, and air permeability (PPS “porosity”) of the coated papers were measured. The brightness of the coated papers was measured using a Technidyne Brightness meter, TAPPI procedure T 452 om-92. Gloss was measured using a Hunter 75° glossmeter according to standard TAPPI procedure T 480 OM-92. The surface smoothness and air permeability of the sheets were measured using a Parker Print Surf (PPS) tester (TAPPI T555 pm-94). The optical properties were analyzed using ANOVA table analysis.

The contact angles of water droplets on the calendered coating papers were measured using a First 10 Angstrom Dynamic Contact Angle measuring device. The calendered coated papers and commercial coated inkjet papers were printed on an Epson Stylus Pro photo realistic inkjet printer and a Hewlett-Packard 820C inkjet printer, using a proprietary test print pattern created with Adobe Photoshop and PageMaker. The ink density and ink gloss of the samples were then measured. The ink density was measured using an X-rite 408 densitometer. The ink gloss of the black ink and delta gloss were measured using a Gardener 60° Micro-Gloss meter. The fidelity of magenta dots was measured at 10% tone scale using a Hitachi HV-10 camera (Hitachi Denshi, Ltd, Japan). Image-Pro plus (version 3.0) was used for measuring the roundness.

The surface properties of the dry coating structure were characterized using a scanning electron microscope (SEM). The pore volume and pore size distribution of the coated papers were measured using a Micromeritics Mercury Intrusion Porosimeter.

RESULTS AND DISCUSSION

For the optical properties of the uncalendered samples, the highest brightness values were obtained for the fumed silica (A) coating. The brightness of all the samples increased with coat weight (Figure 3). The gloss of the fumed silica coatings (A and B) was higher than the gloss of the fumed alumina coating, prior to calendering. As with brightness, the gloss of all the samples increased with coat weight.

The most significant optical property improvements with calendering were found in gloss and smoothness (Figures 4-5). The results indicate that the specular reflection of the alumina-coated surface is sufficient to provide gloss comparable to commercially coated glossy inkjet papers if the alignment of the particles and smoothness of the coating layer are improved by calendering. The 75° gloss of the three commercial glossy inkjet papers ranged from 65-90%. The gloss values of the silica coatings were also increased significantly, but not as much as for the alumina coating. The differences in the gloss values before and after calendering and between the two silicas indicate a difference in the internal structure of the coating layers, which is attributed to the differences in their particle sizes. Typically, small pigments and a narrow pigment size distribution produce more gloss, due to the ability of the smaller pigments to fill the surface irregularities, providing a smoother surface with more compact air boundary surfaces. However, the opposite is found in this case. The gloss and smoothness of the larger particle fumed silica A was higher. The causes of these differences were revealed by the later inspection of the coating surfaces with a scanning electron microscope. Inspection of the surfaces of the two coatings revealed the presence of coating cracks in the fumed silica B sample (Figures 6-8). It is believed that the cracks are the results of binder shrinkage, a known polyvinyl alcohol/silica phenomenon. Due to the greater surface tension forces between the smaller particles of silica B during drying, more cracks are formed in its coating layer, which detrimentally decreased its gloss. The difference between the gloss of the alumina and silica pigments of comparable size is the result of the difference in the refractive index of the two pigments (9). The refractive index of alumina is well known to be higher than the refractive index of silica (10).

Although calendering significantly improved the gloss of the coatings, calendering is not always desirable in this application, because it can have the negative effect of compressing the coating layer. Compression of the coating layer reduces the pore volume in the coating layer, adversely affecting the rate of liquid absorption (ink receptivity) and, consequently, can reduce print quality. As indicated in Figure 9, air permeability decreased with calendering.

Dynamic contact angle measurements and printing studies on the calendered samples were performed to determine if the rate of liquid absorption and print quality were adversely affected. The dynamic contact angle of each sample was measured and compared to three commercial inkjet papers, two glossy and one matte, to determine the rate of liquid absorption and to study the influence of pigment type on the surface tension of the sheet. As seen in Figures 10-12, the contact angles decreased with increasing coat weight. This corresponds to the air permeability results, which showed the air permeability to also decrease with coat weight (calendered samples). Comparison of these figures show the initial contact angle of the alumina coating to be higher than the silica pigments, indicating a greater interaction between the surface and test fluid (distilled water). The differences in surface interactivity with water were found to be even greater than the alumina, for the commercial papers tested (Figure 13). This is not surprising since no cationic polymers or coating additives were added to our coatings and the presence of such additives would have a pronounced affect on the interactivity of the surface.

The dynamic contact angle measurements also show significant differences in the rate of liquid absorption between the commercial papers and coated calendered samples produced in this study. The fumed pigments were all more absorptive than the commercial samples. It was observed that these samples also dried faster after printing. The commercial papers were prone to ink setoff and had to be handled carefully after printing, while the fumed alumina and silica samples could be handled immediately. Tests to quantify the drying properties of the sheet were attempted, and resulted in the development of a new ink drying test method (11).

The ink density of the calendered samples and commercial samples are presented in Figures 14-19. The results for the Epson printer were quite different from those for the HP printer. For all calendered paper samples, the ink densities of the HP printed samples were higher than those of the Epson printed samples. For both printers, the ink density of the black ink was higher than the density of the cyan, magenta, or yellow inks. The differences between the ink densities of both fumed silica coated papers and commercially produced papers are small.

The black ink gloss of the HP printed samples was higher than that on the Epson printer samples (Figure 20-21). The ink gloss of the fumed silica (B) coated paper was higher than that of the other samples. Delta gloss is the difference between the ink gloss and the paper gloss. Positive or zero values of delta gloss indicate that coating gloss is not lost when it contacts the ink. Table 4 shows delta gloss for the black ink. The delta gloss of fumed silica (A) and (B) samples had some positive values, indicating that they maintain or enhance their coating gloss when contacted by the ink. These results are quite different from the fumed alumina results, which are negative in value, indicating that the coating gloss is higher than the ink gloss. Comparison of the delta gloss values to the coating gloss values (not shown), measured at the same angle of incidence, show the loss in ink gloss for the alumina samples to range from +10 to -25% depending on the coat weight. The delta gloss of the commercially printed inkjet papers were almost negative ranging from +5 to -25% for the Epson printer and from +8 to -23% for the HP printer. Thus, the fumed silica and aluminum coated papers are better than or comparable to the commercial papers in ink gloss behavior.

Table 4. Delta Gloss of Each Sample (Black)

[Epson Printer]

Fumed alumina		Fumed Silica(A)		Fumed Silica(B)	
Coat Weight (g/m ²)	Delta Gloss	Coat Weight (g/m ²)	Delta Gloss	Coat Weight (g/m ²)	Delta Gloss
6.5	-8.90	6.8	-3.08	6.1	-0.18
9.1	-9.30	9.8	-2.99	8.9	-0.68
11.1	-9.30	12.8	-3.13	12.1	0.52
15.5	-8.68	16.3	-2.20	16.5	0.86

[Hewlett Packard Printer]

Fumed alumina		Fumed Silica(A)		Fumed Silica(B)	
Coat Weight (g/m ²)	Delta Gloss	Coat Weight (g/m ²)	Delta Gloss	Coat Weight (g/m ²)	Delta Gloss
6.5	-9.12	6.8	-1.94	6.1	1.42
9.1	-8.73	9.8	-2.67	8.9	0.18
11.1	-9.56	12.8	-0.05	12.1	1.24
15.5	-8.90	16.3	1.23	16.5	1.34

The dot fidelity results for magenta dots are shown in Figures 22-24. Dot fidelity includes the area of dots and dot roundness (12). Roundness is one of the most important factors of print quality, because it represents the shape of the dot relative to a perfect circle. If the roundness is 1, it means the dots are perfect circles. Values of roundness greater than 1.0 actually indicate lack of roundness. Therefore, the closer the value of roundness is to 1, the better the quality of dots. The absolute area of a printed dot is important, because it represents the actual resolution of the printer, as opposed to the manufacturer's quoted resolution. The dot area should be as small as possible, while still being able to fill a solid area. The smallest space-filling dot has a diameter $\sqrt{2}$ times the spacing between dots (13). For example, the smallest diameter for a 300 dot per inch printer would be 120 μm . Any dots larger than this will only decrease the sharpness of the image without contributing significantly to the print density.

In essentially all of the cases, the roundness and dot diameter decrease with increasing coat weight (Figures 22-24). The dot diameters are all a factor of 2-3 larger than the smallest space-filling size discussed above (120 μm for the HP at 300 dots per inch and 50 μm for the Epson at 720 dots per inch).

The pore size distributions of the fumed silica (A and B) and fumed alumina produced papers are compared to that of commercial papers in Figures 25-27. The pore size distributions of the fumed pigments are much different from those of commercial papers. The incremental intrusion of the commercial glossy papers was different from that of fumed pigments samples because their pore structures consist of multiple coating layers.

CONCLUSIONS

The optical properties, brightness and gloss, were affected by pigment type and coat weight. The correlation between improvements in optical properties and smoothness indicate that the property improvements were due to an increase in surface coverage with coat weight. Air permeability (PPS porosity) decreased with coat weight.

The substantial increase in gloss with calendering for the fumed pigments demonstrates that the particle sizes of the fumed pigments are sufficient to produce a high gloss inkjet coating.

Print quality, as measured by ink density, ink gloss, delta gloss, and roundness was strongly dependent on pigment type and correlated well with air permeability results. Coat weight did not significantly affect these properties. The difference in print quality between the two printers indicates differences between the two inking systems.

SEM photographs revealed the presence of coating cracks. Regardless of the pigment type, cracks were present. However, the cracks were larger for the pigment of smaller particle size, fumed silica B.

The mercury porosimetry data showed the pore size distribution of the two fumed silica samples were similar to one another, even though the particle sizes of the pigments were different. The pore size distribution of the alumina coating differed significantly from the silica coatings. The pore size distribution for both fumed pigments differed significantly from the commercial samples.

REFERENCES

1. Kulmala, A., Paulapuro, H. and Oittinen, P., "Paper requirements for electrophotographic printing," IS&T NIP10, 10th International Congress on Advances in Non-Impact Printing Technologies, Springfield VA, 1994, pp. 466 - 470.
2. Chapman, D.M., "Silica-Gel coatings for ink-jet media," Grace Davison (internal document), Baltimore, MD.
3. Withiam, M. C., "Silica Pigment Porosity Effects on Color Inkjet Printability", IS&T, NIP12, 12th International Congress on Advances in Non-Impact Printing Technologies, pp 409-417.
4. Boothby, C., "New technology drives global coating trends," PIMA Papermaker, May 1997, pp. 38-45.
5. Boylan, J.R., "Using polyvinyl alcohol in inkjet printing paper," TAPPI, 80(1): 68 – 70, 1997
6. Londo, Mike., "On-machine coating of inkjet paper possible with modified kaolin," Pulp and Paper, May 2000, pp. 37-43.
7. Omura, Tomonobu., Ueno, Takashi., and Limori, Yoshifumi., "Glossy inkjet media by cast-coating method", Proceeding of the 1998 Pan-Pacific and International Printing and Graphic Arts Conference, 1998, pp. 169-174.
8. Asano, Shinichi. *et al.*, U.S patent 5670242 (September 23, 1997).
9. Lee, D. I., " A Fundamental Study on Gloss", TAPPI Coating Conference, 1974, pp.97-103.
10. Dean, Trevor., "The Essential Guide to Aqueous Coating of Paper and Paperboard", PITA,1997, pp.3.1-3.66.
11. Thummala, Vinay., Joyce, Margaret and Fleming, P. D., "A Near Infrared Drying Technique for Measuring Inkjet Drying Time", In Preparation.
12. Sarafano, J. and Pekarovicova, A., "Factors Affecting Dot Fidelity in Solvent Based Publication Gravure", American Ink Maker, 77, 732-36 (1999).
13. Cawthorne, James., Fleming, Paul D., Mehta, Falguni, Halwawala, Saurabh and Joyce, Margaret, "Interpretation of Dot Area and Dot Shape based on Image Analysis", In Preparation.

Acknowledgement

We appreciate Wausau Paper Company (Otis, Maine) for supplying the base paper for this study.

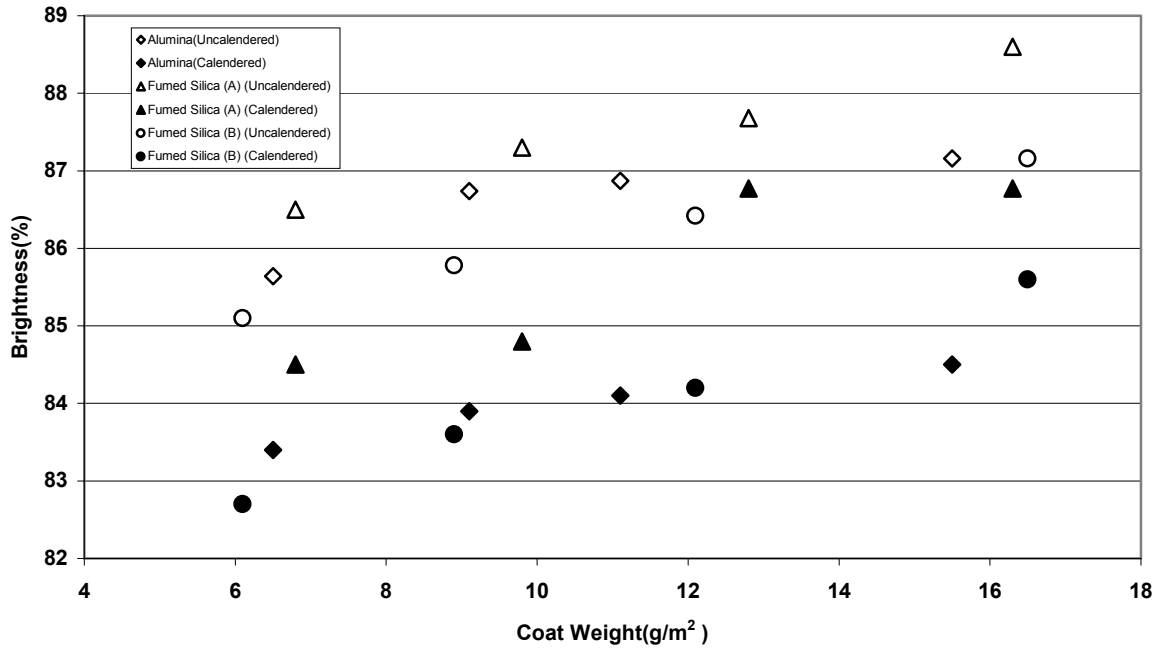


Figure 3. Influence of Pigment on Brightness

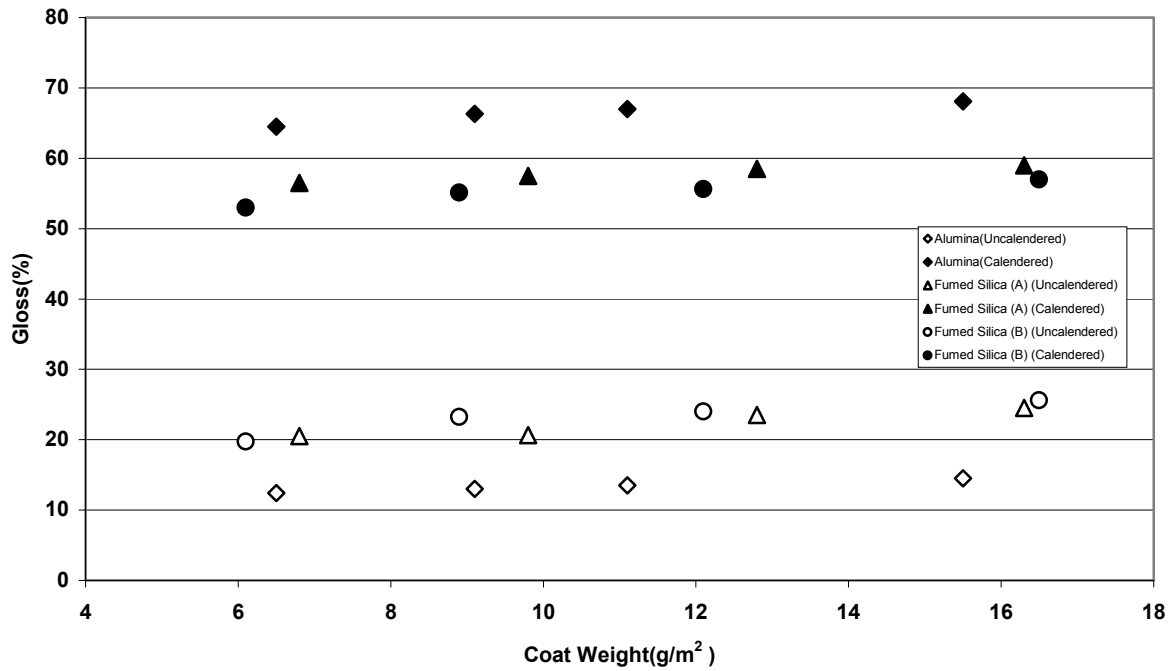


Figure 4. Influence of Pigment on Gloss

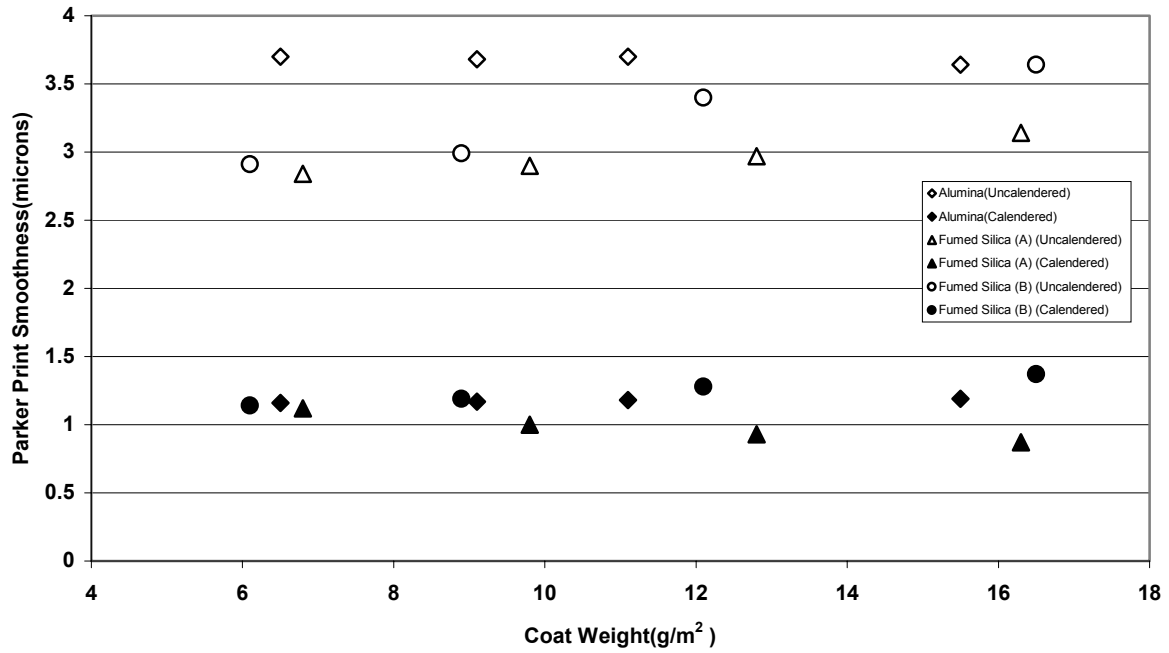
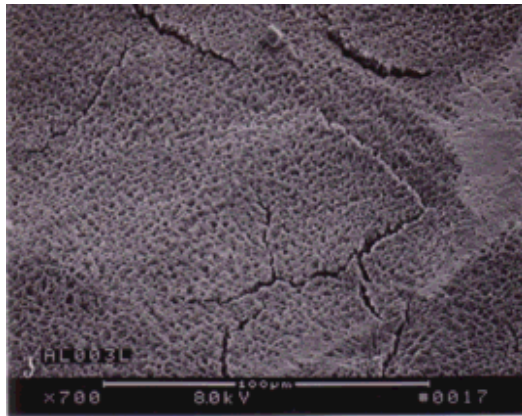
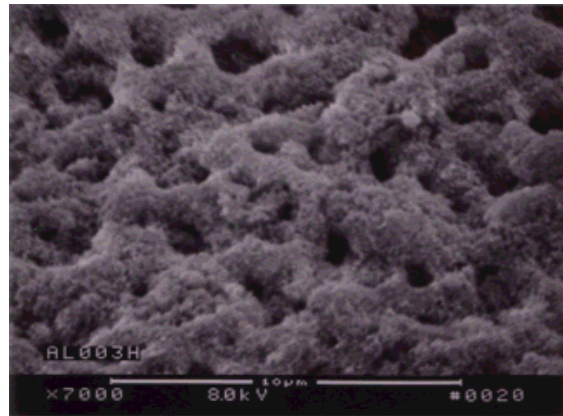


Figure 5. Influence of Pigment on Smoothness

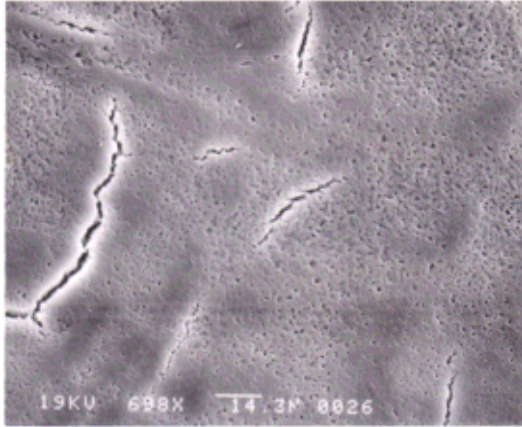


(700x magnifications)

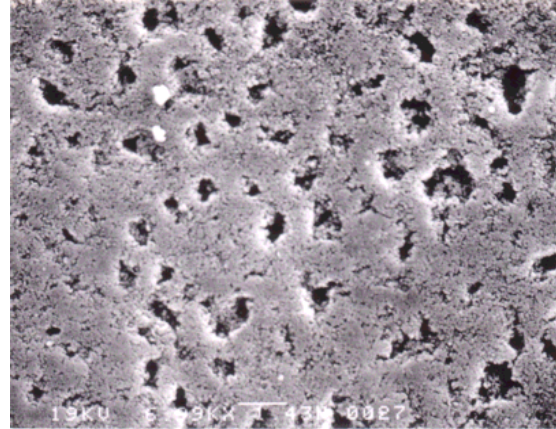


(7000x magnifications)

(Uncalendered Samples)



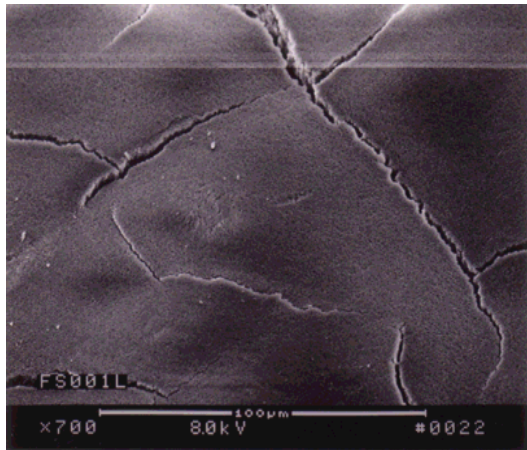
(700x magnifications)



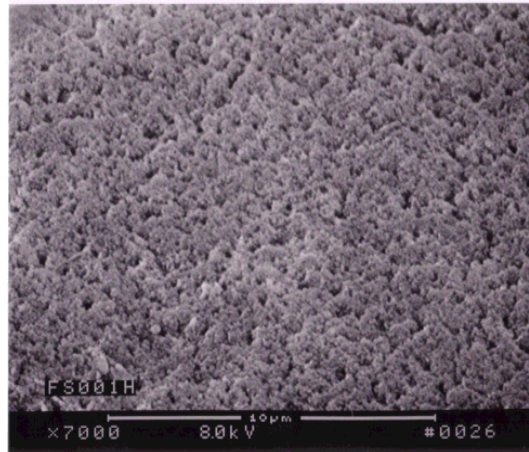
(7000x magnifications)

(Calendered Samples)

Figure 6. SEM Pictures of Alumina (Coat weight: 6 g/m²)

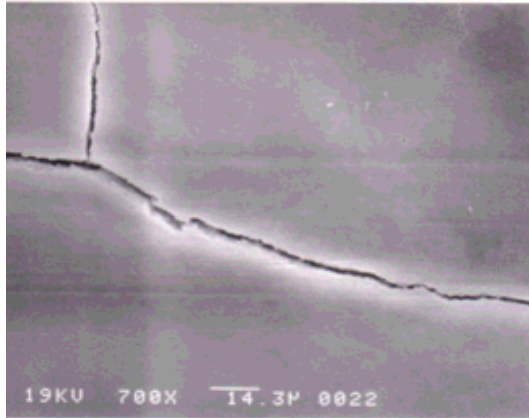


(700x magnifications)

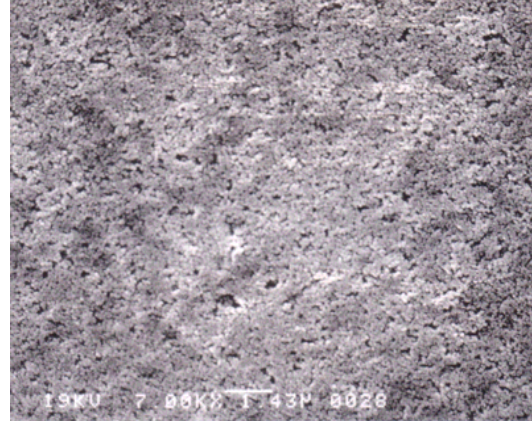


(7000x magnifications)

(Uncalendered Samples)



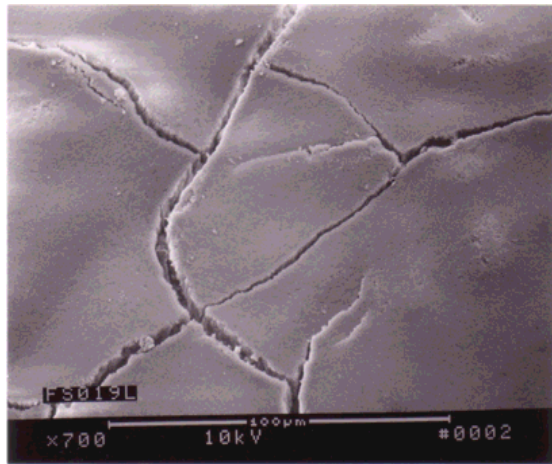
(700x magnifications)



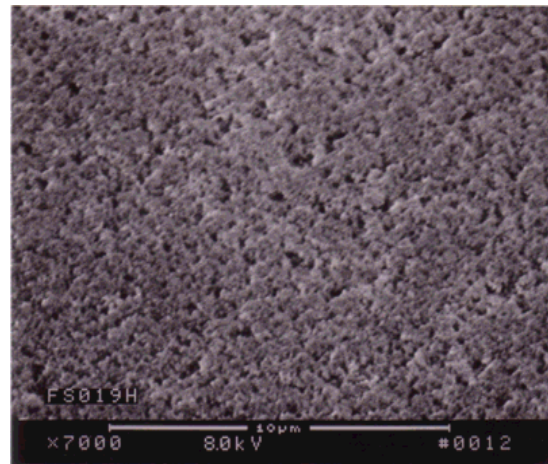
(7000x magnifications)

(Calendered Samples)

Figure 7. SEM Pictures of Fumed Silica (A) (Coat Weight: 6 g/m²)

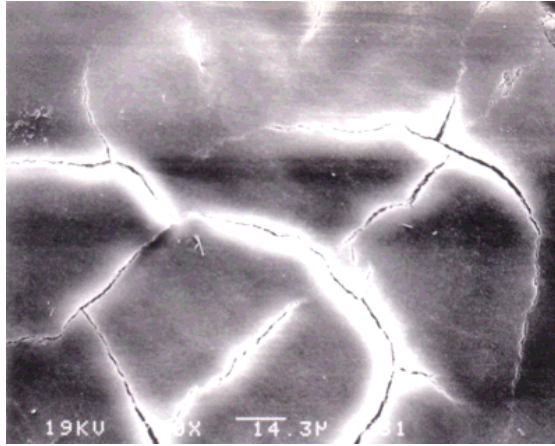


(700x magnifications)

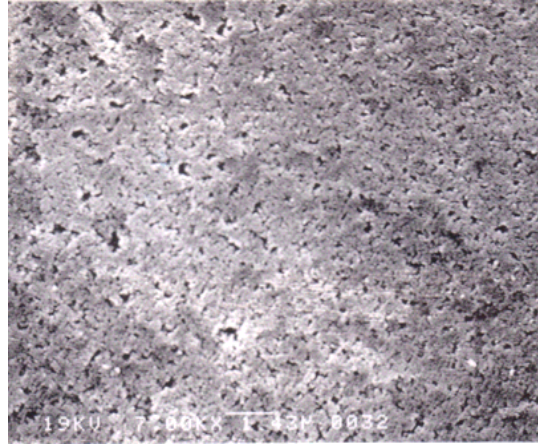


(7000x magnifications)

(Uncalendered Samples)



(700x magnifications)



(7000x magnifications)

(Calendered Samples)

Figure 8. SEM Pictures of Fumed Silica (B) (Coat Weight: 6 g/m²)

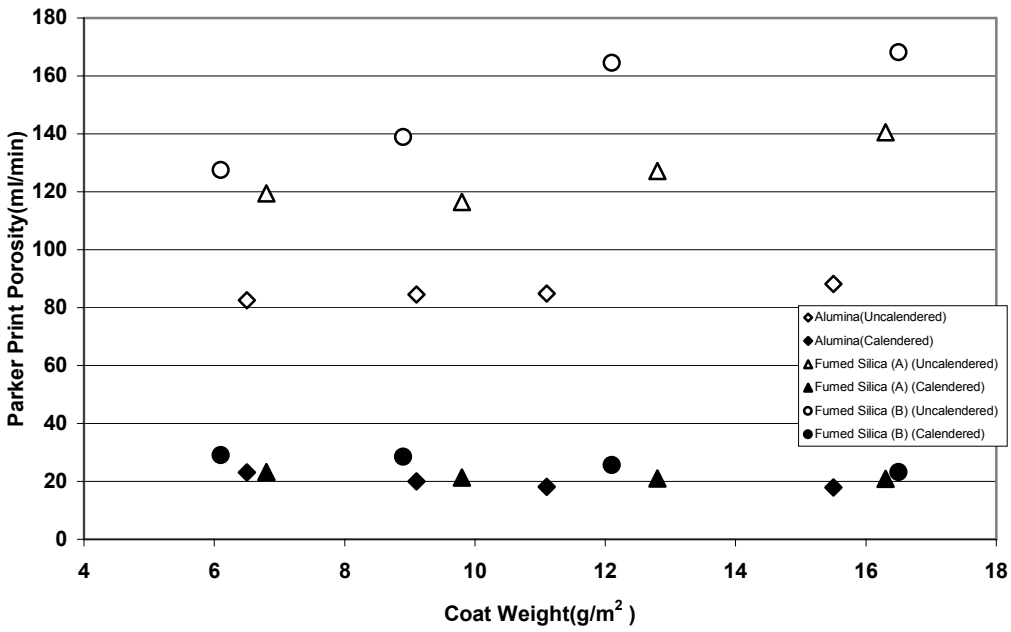


Figure 9. Influence of Pigment on Air Permeability

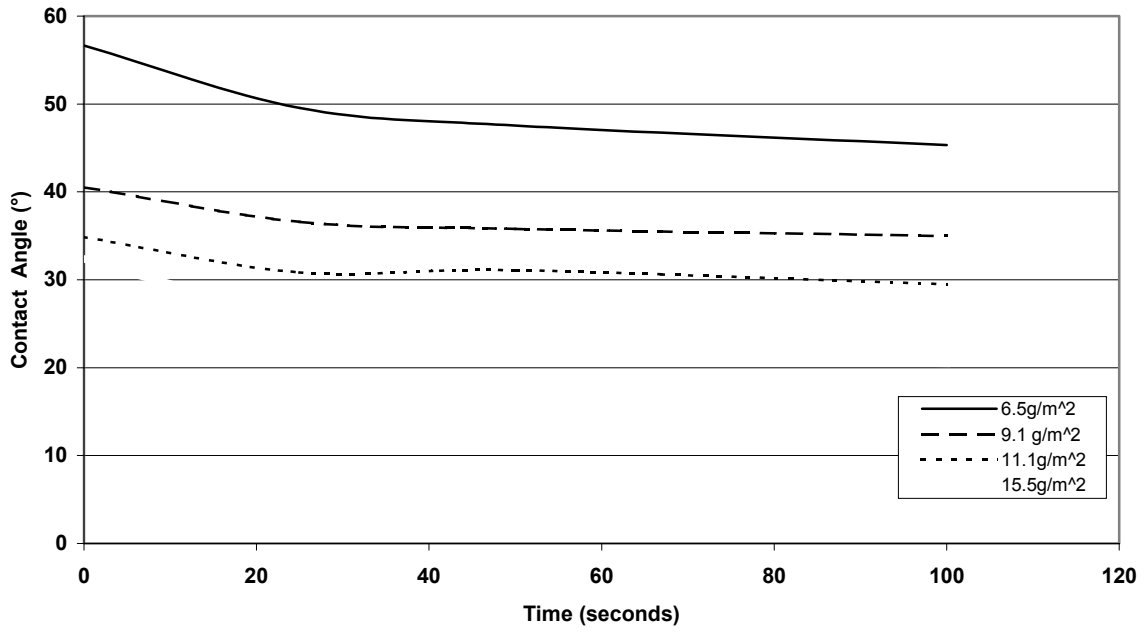


Figure 10. Contact Angle of CLC Coatings of Alumina

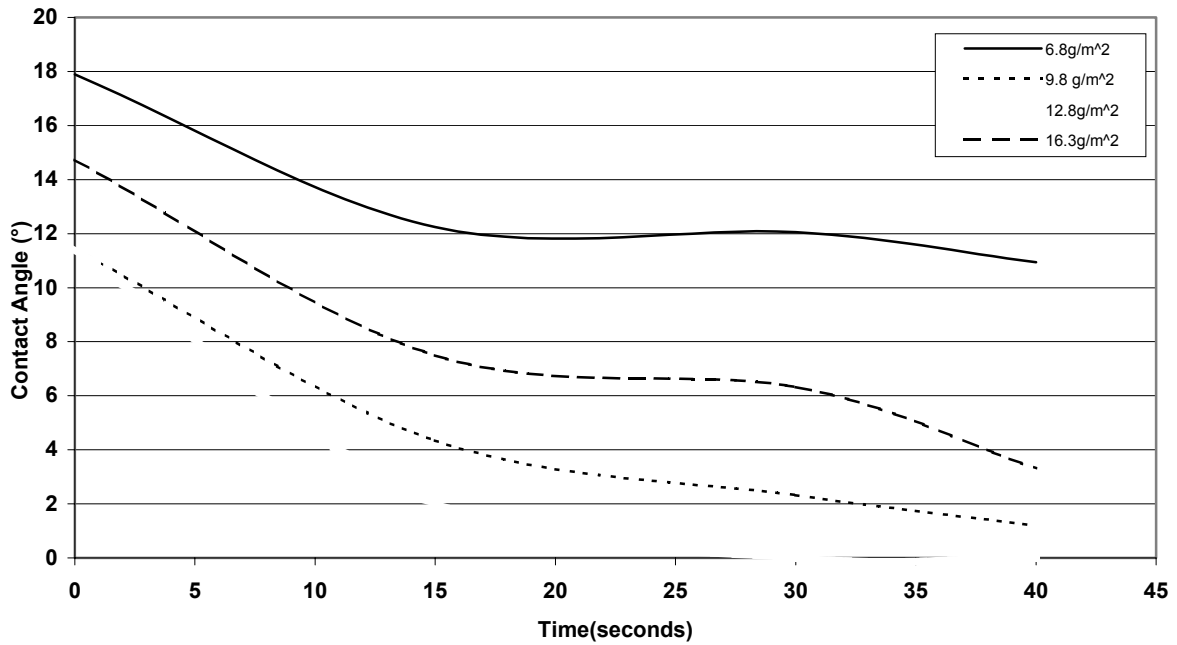


Figure 11. Contact Angle of CLC Coatings of Fumed Silica (A)

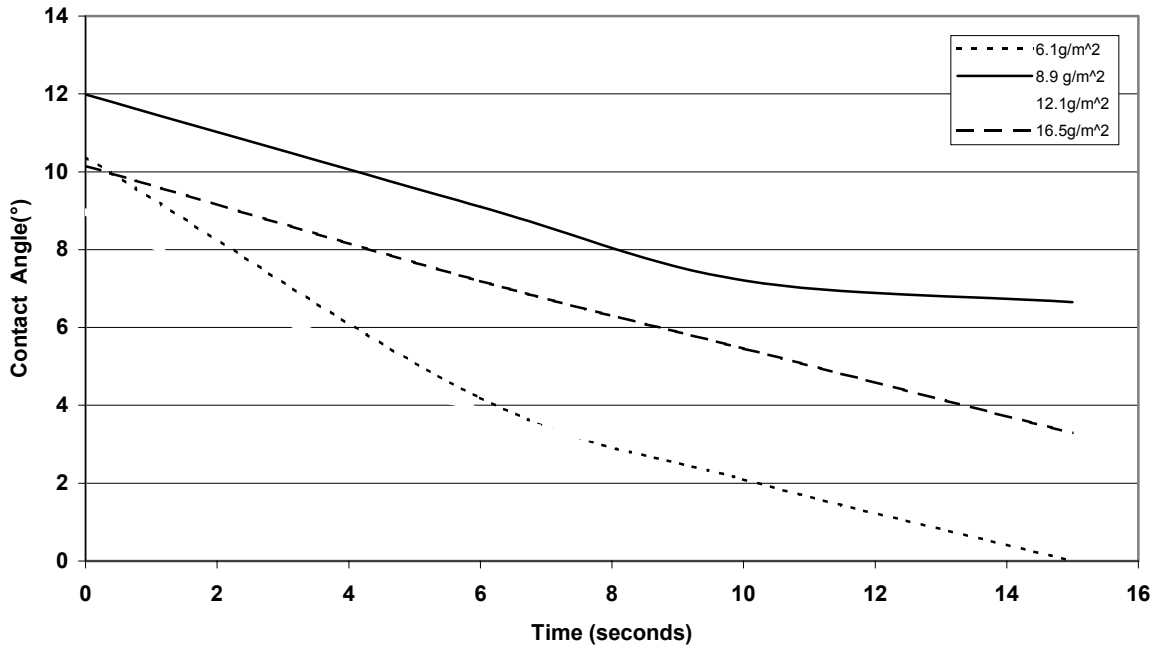


Figure 12. Contact Angle of CLC Coatings of Fumed Silica(B)

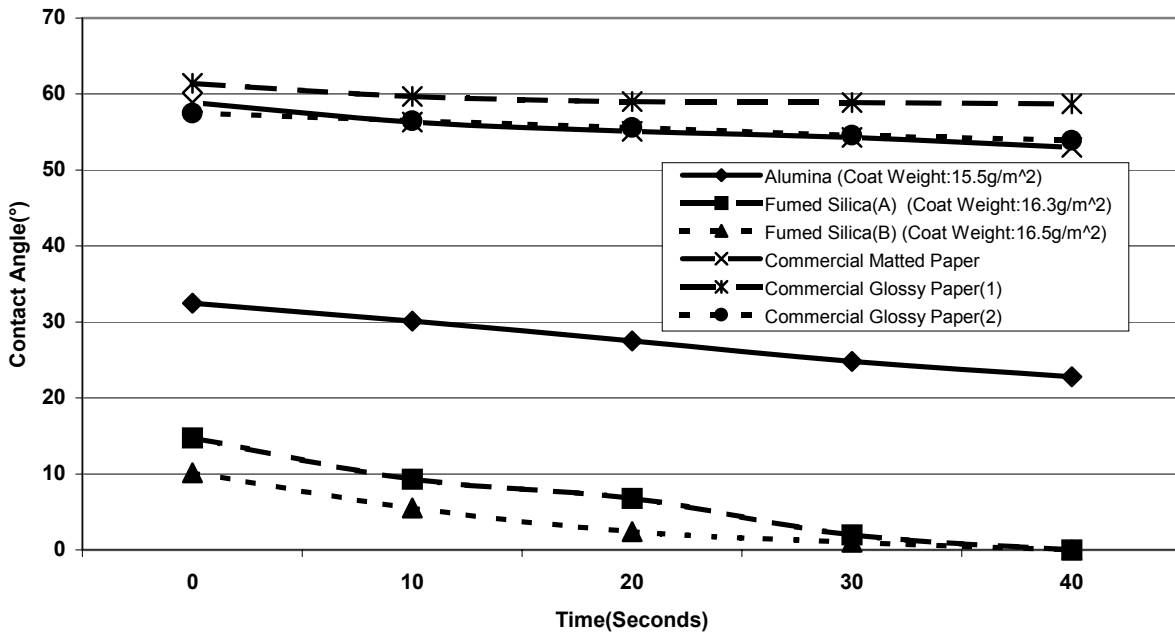


Figure 13. Contact Angle Comparison of Fumed Pigments and Commercial Papers

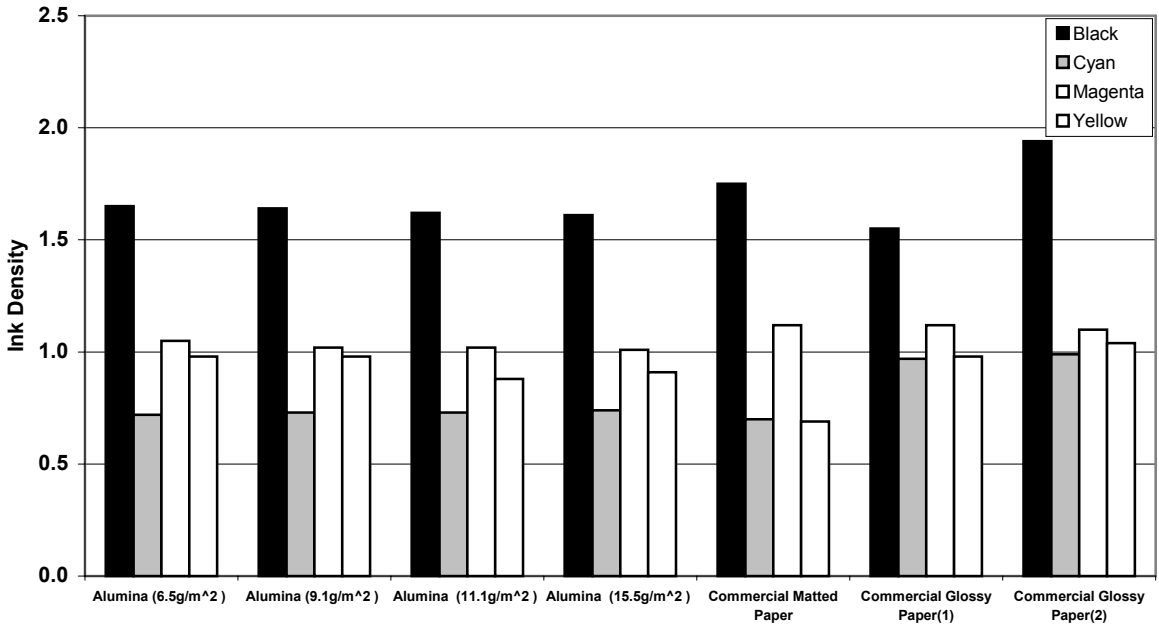


Figure 14. Ink Density Comparison of Each Samples[Epson Printer]

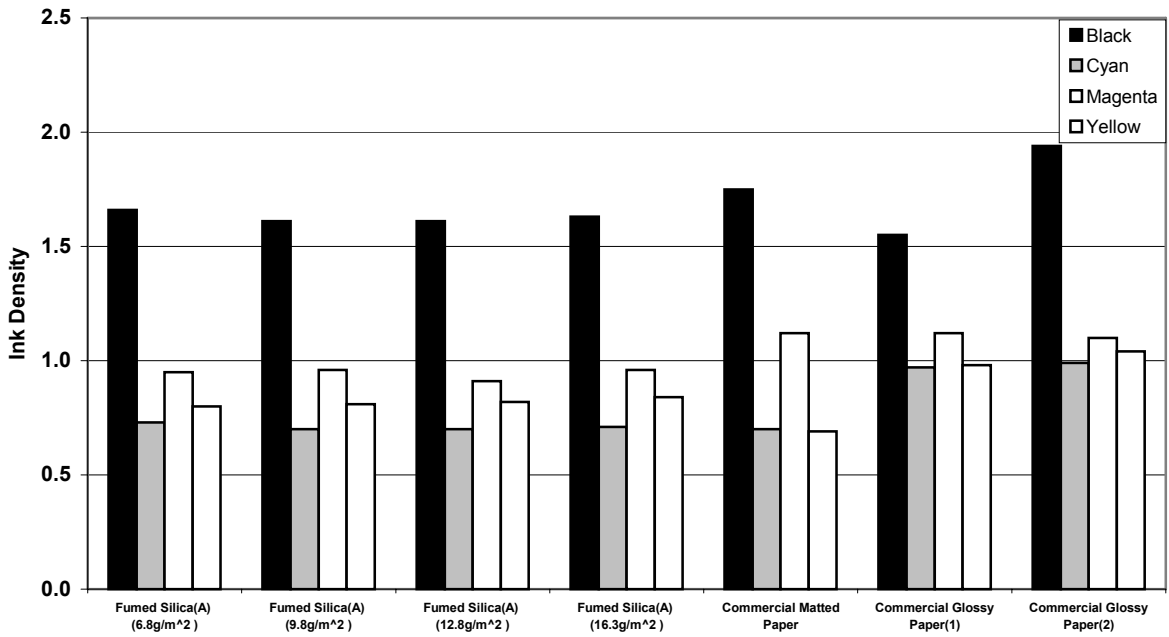


Figure 15. Ink Density Comparison of Each Sample[Epson Printer]

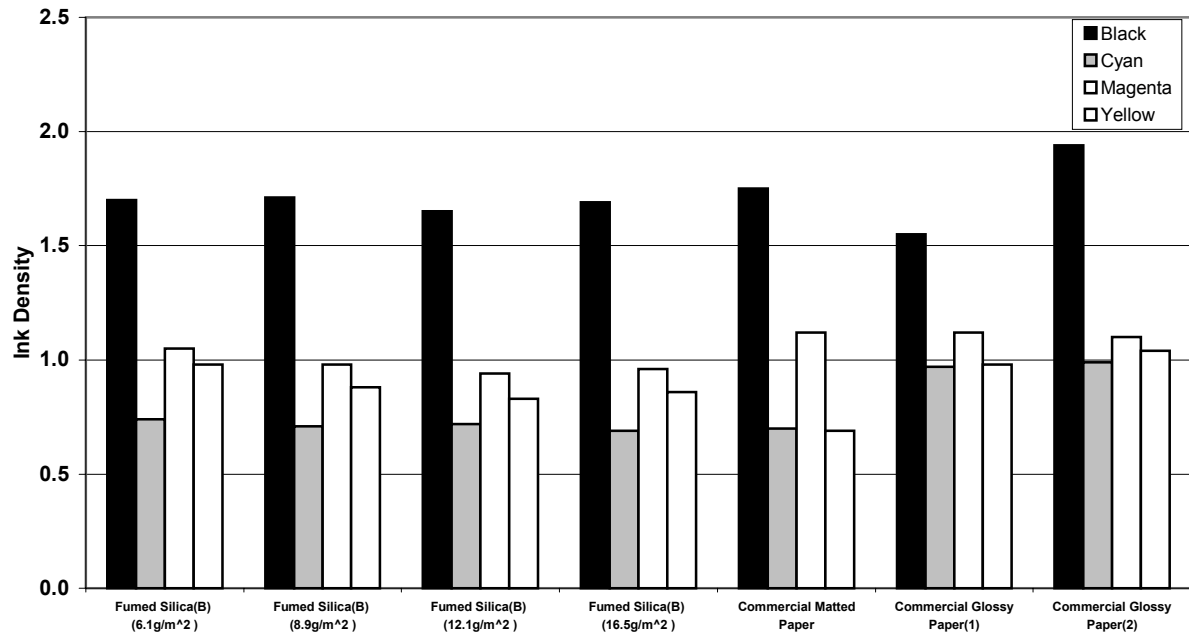


Figure 16. Ink Density Comparison of Each Sample[Epson Printer]

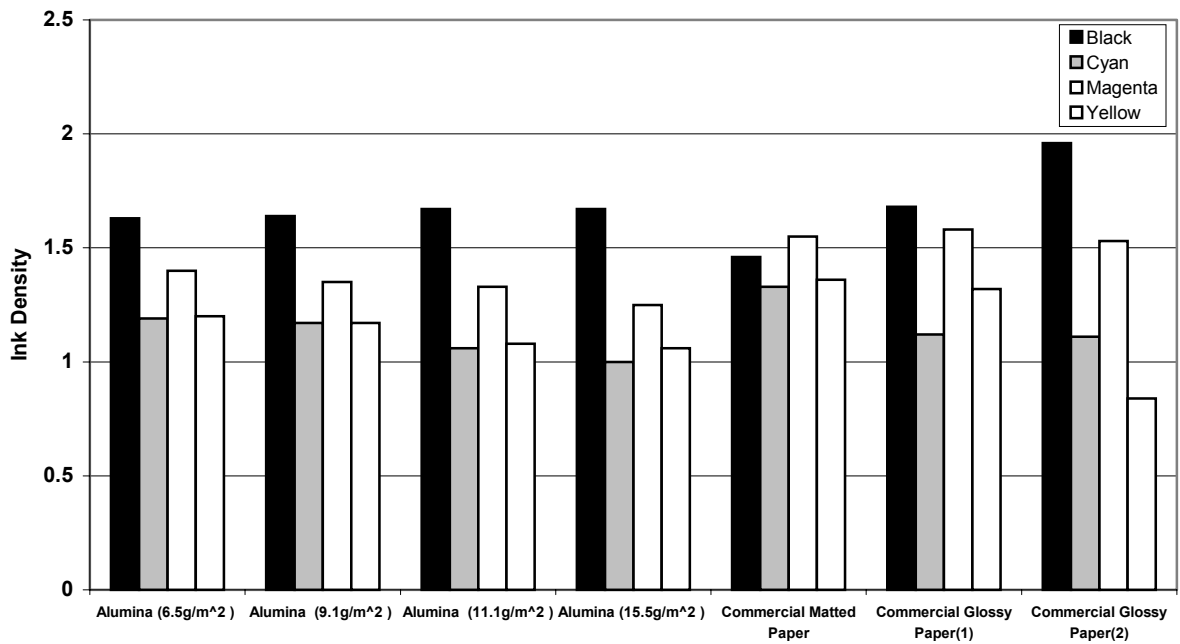


Figure 17. Ink Density Comparison of Each Sample[Hewlett Packard Printer]

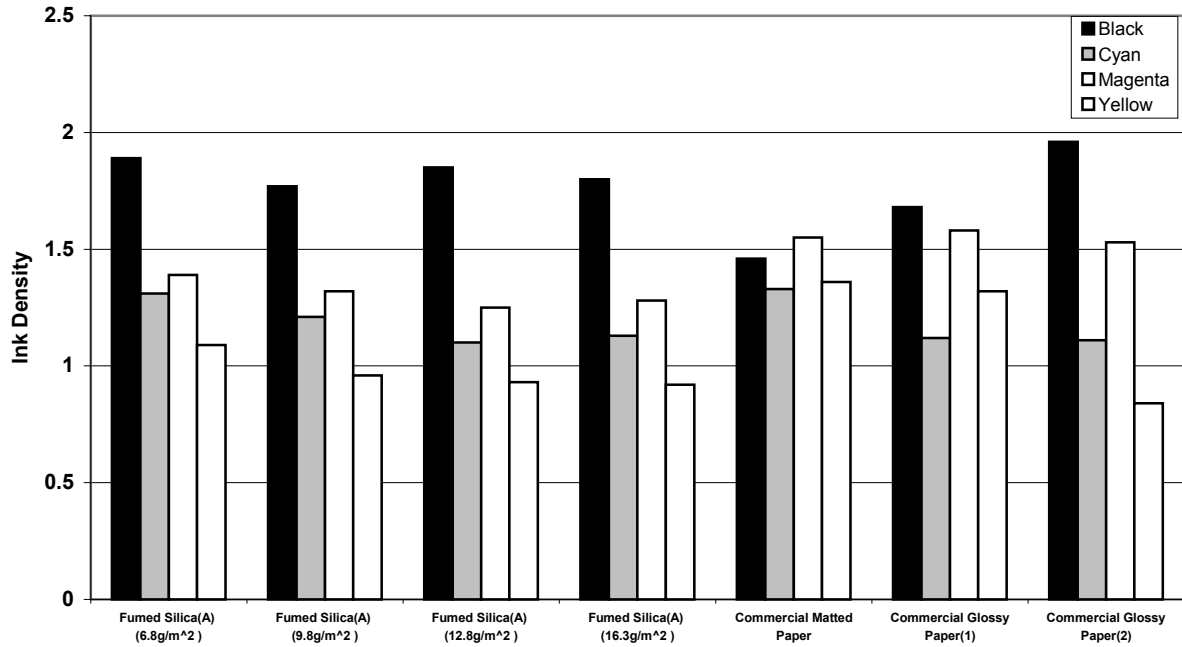


Figure 18. Ink Density Comparison of Each Sample[Hewlett Packard Printer]

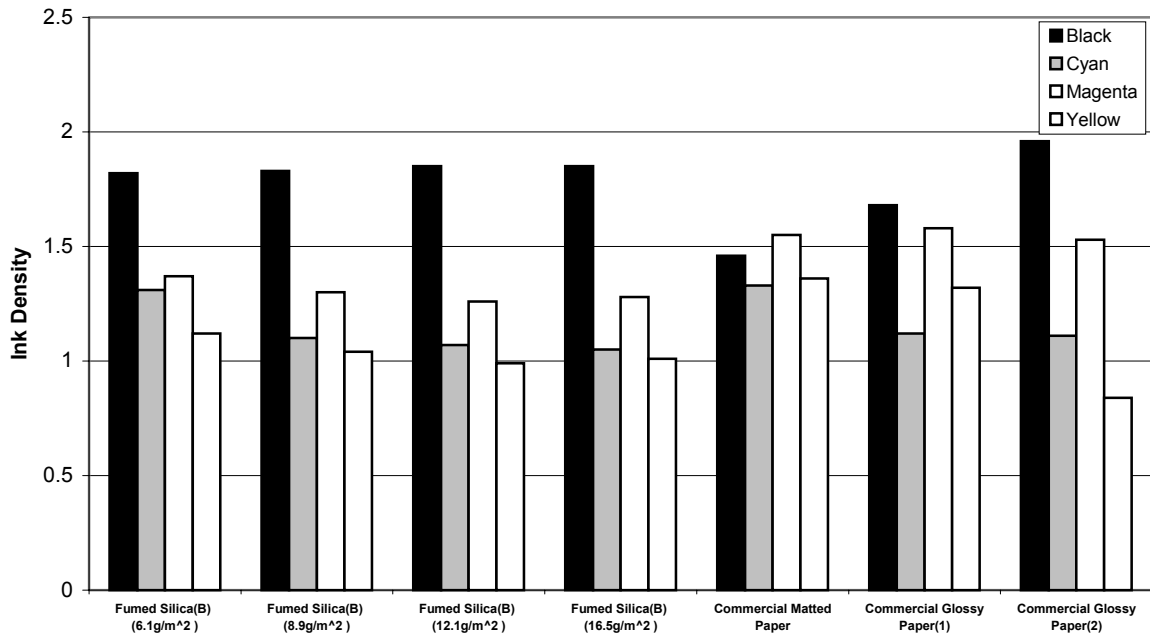


Figure 19. Ink Density Comparison of Each Sample[Hewlett Packard Printer]

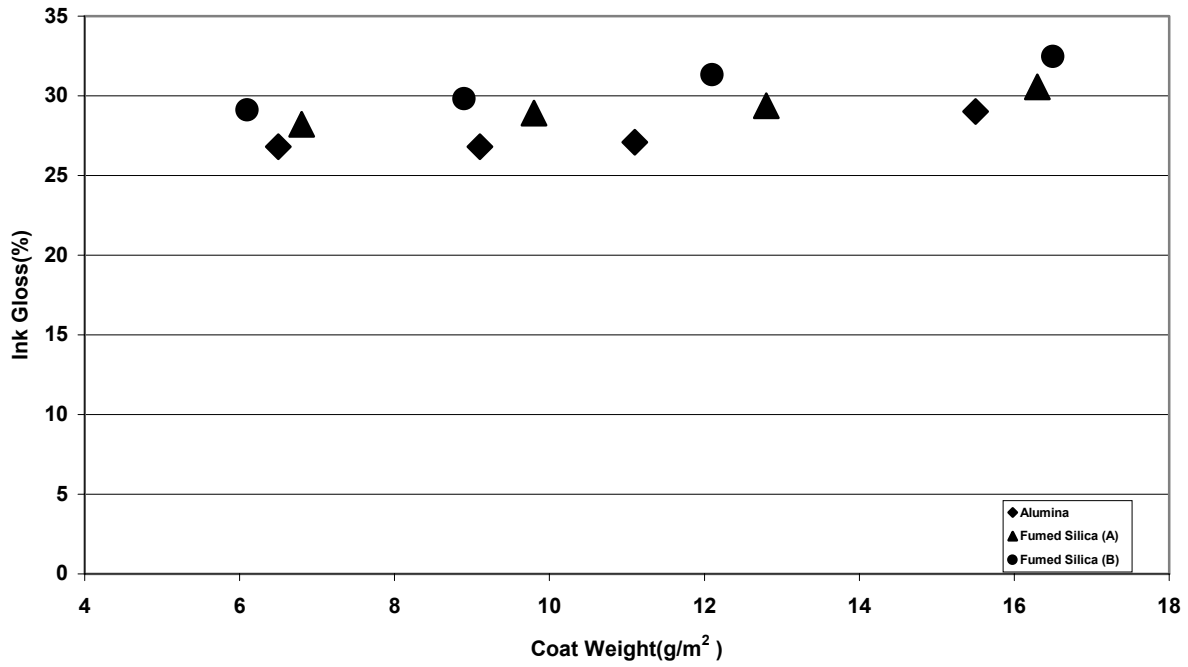


Figure 20. Ink Gloss Comparison of Each Sample[Black, Epson Printer]

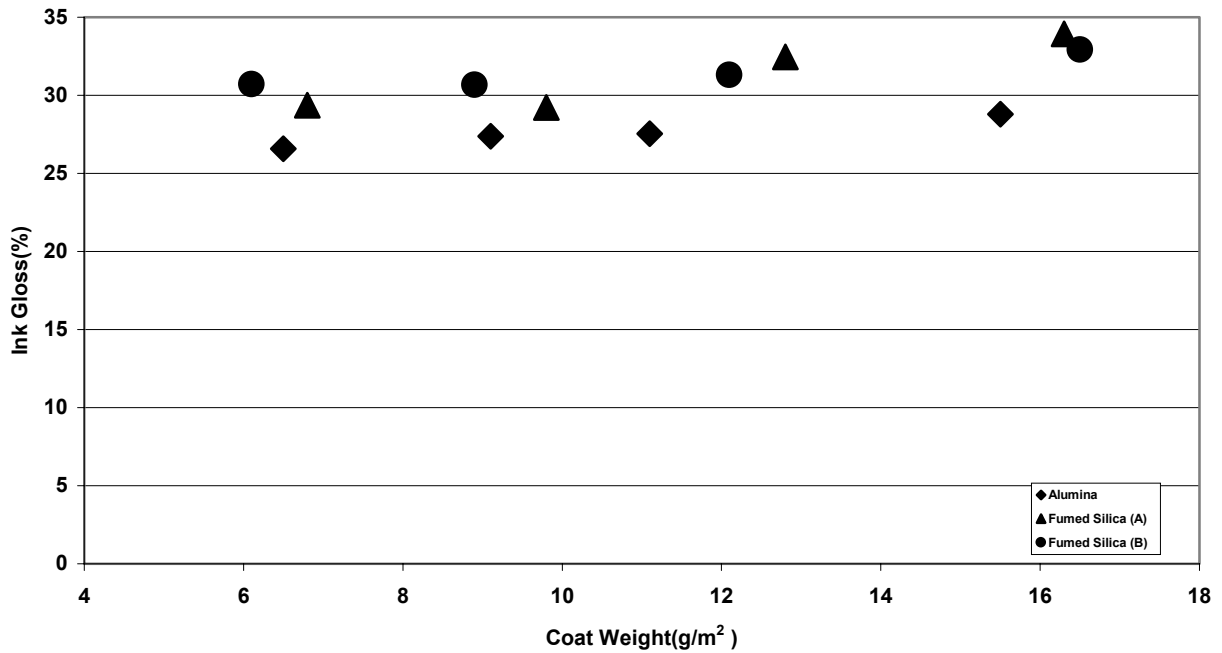
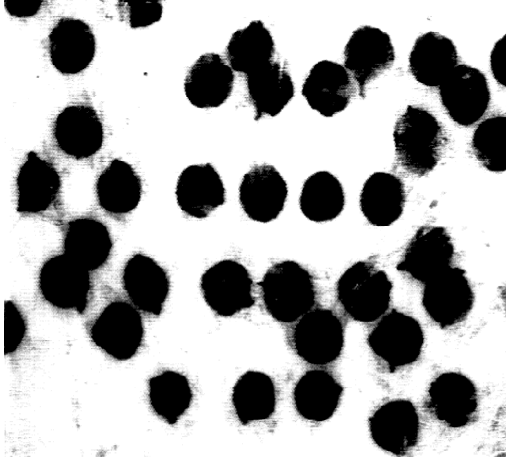


Figure 21. Ink Gloss Comparison of Each Sample[Black, Hewlett Packard Printer]

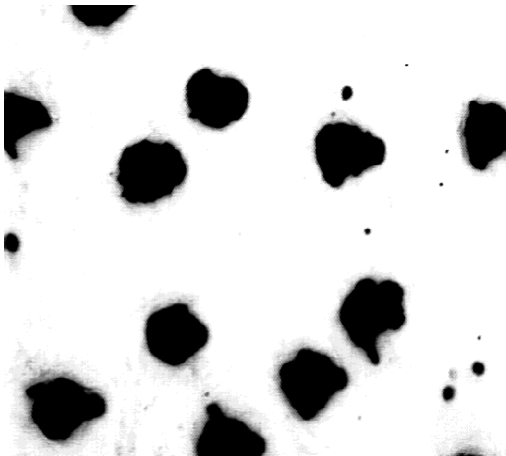


(Roundness=1.20, Standard deviation: 0.39)
(Diameter= 192 μ)

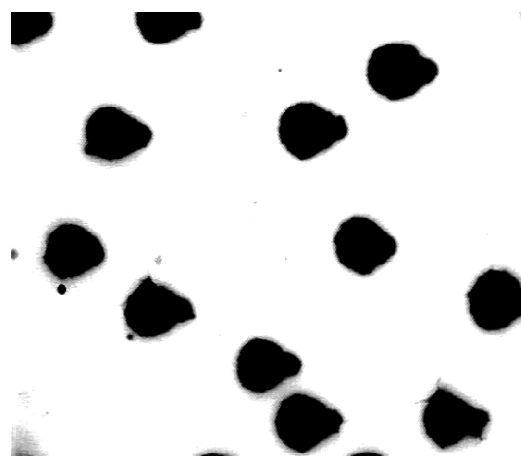


(Roundness=1.12, Standard deviation: 0.26)
(Diameter= 169 μ)

(A) Epson Printing Samples(Coat weight; left: 6.5 g/m², right: 15.5 g/m²)



(Roundness=1.25, Standard deviation: 0.21)
(Diameter= 237 μ)



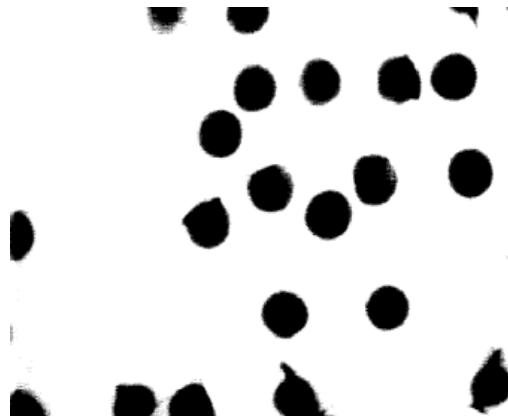
(Roundness=1.17, Standard deviation: 0.30)
(Diameter= 216 μ)

(B) Hewlett Packard Printing Samples(Coat weight; left: 6.5 g/m², right: 15.5 g/m²)

Figure 22. Printing Dots of Alumina Samples(Color: Magenta)



(Roundness=1.28, Standard deviation: 0.45)
(Diameter= 193 μ)



(Roundness=1.08, Standard deviation: 0.04)
(Diameter= 190 μ)

(A) Epson Printing Samples(Coat weight; left: 6.8 g/m², right: 16.3 g/m²)



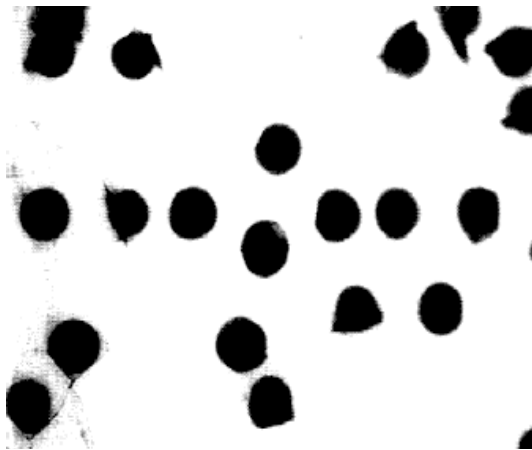
(Roundness=1.16, Standard deviation: 0.11)
(Diameter= 219 μ)



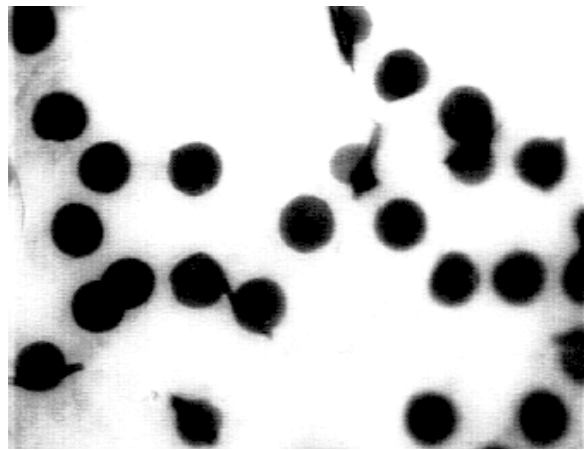
(Roundness=1.14, Standard deviation: 0.08)
(Diameter= 201 μ)

(B) Hewlett Packard Printing Samples(Coat weight; left: 6.8 g/m², right: 16.3 g/m²)

Figure 23. Printing Dots of Fumed Silica(A) Samples(Color: Magenta)

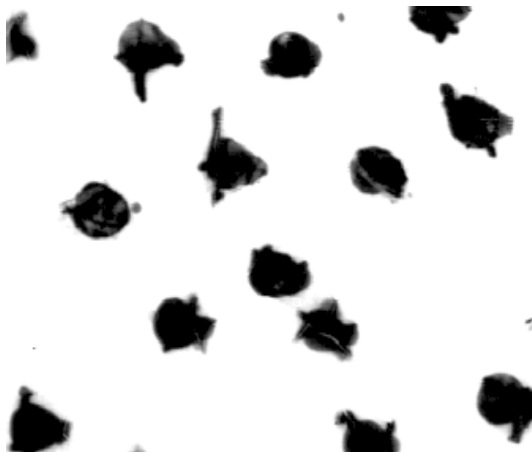


(Roundness=1.23, Standard deviation: 0.17)
(Diameter= 169 μ)



(Roundness=1.25, Standard deviation: 0.23)
(Diameter= 174 μ)

(A) Epson Printing Samples(Coat weight; left: 6.1 g/m², right: 16.5 g/m²)



(Roundness=1.18, Standard deviation: 0.14)
(Diameter= 200 μ)



(Roundness=1.39, Standard deviation: 0.30)
(Diameter= 173 μ)

(B) Hewlett Packard Printing Samples(Coat weight; left: 6.1 g/m², right: 16.5 g/m²)

Figure 24. Printing Dots of Fumed Silica(B) Samples(Color: Magenta)

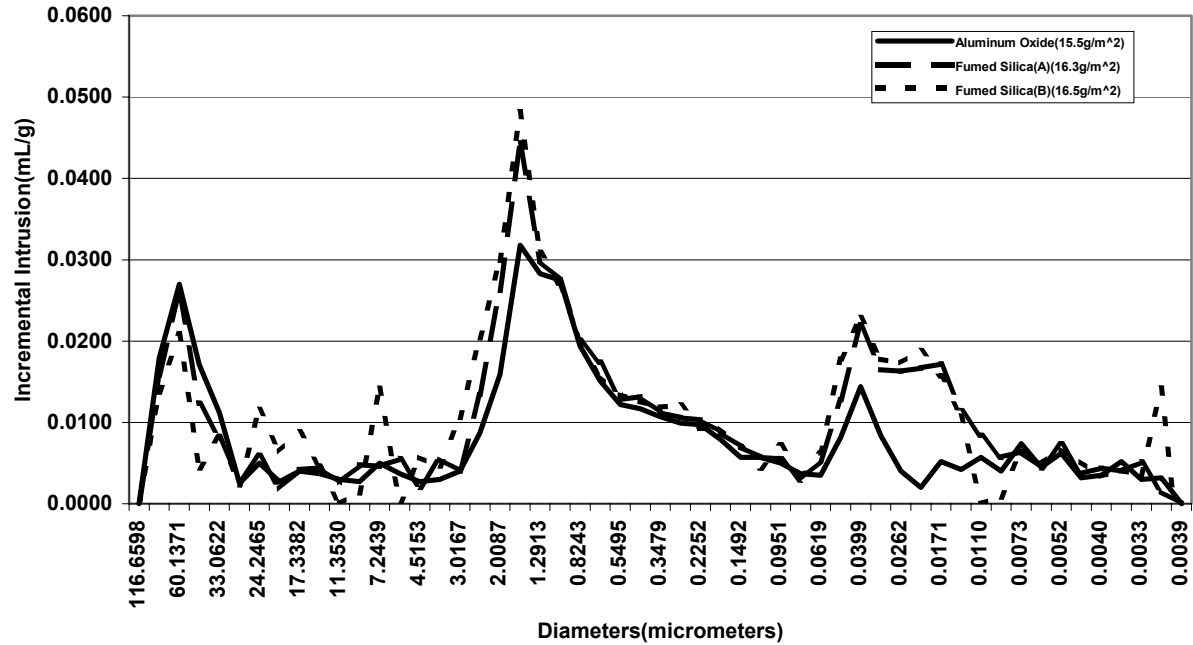


Figure 25. Pore Size Distribution of metallic oxides coatings by Mercury Intrusion Porosimeter

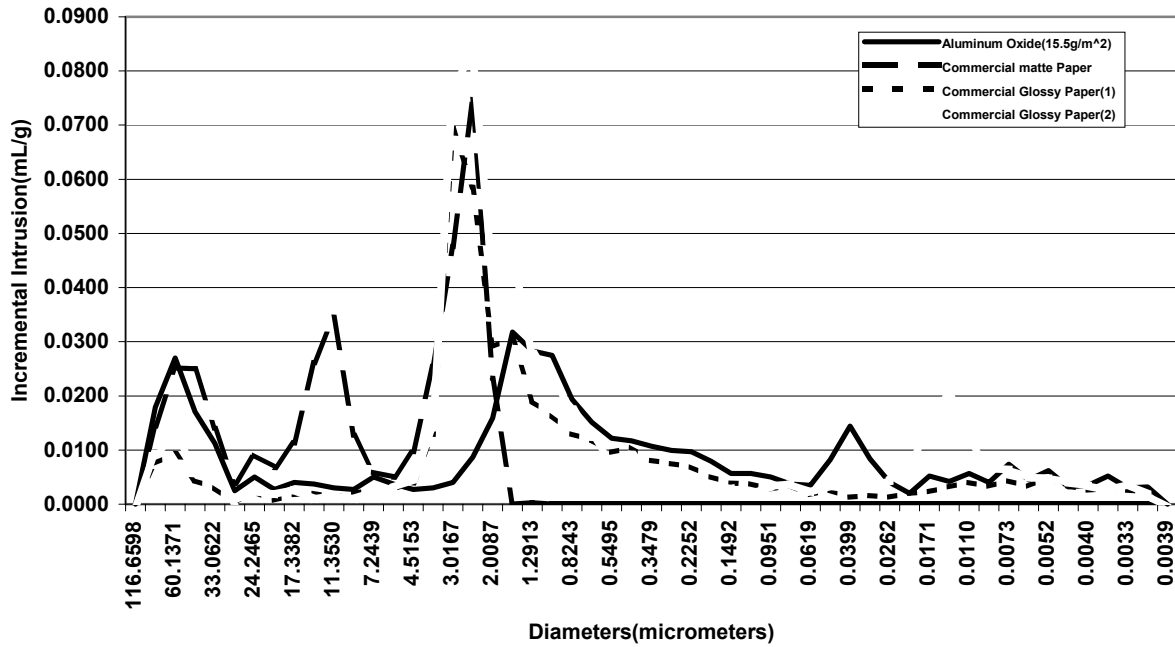


Figure 26. Pore Size Distribution of Alumina and Commercial Papers by Mercury Intrusion Porosimeter

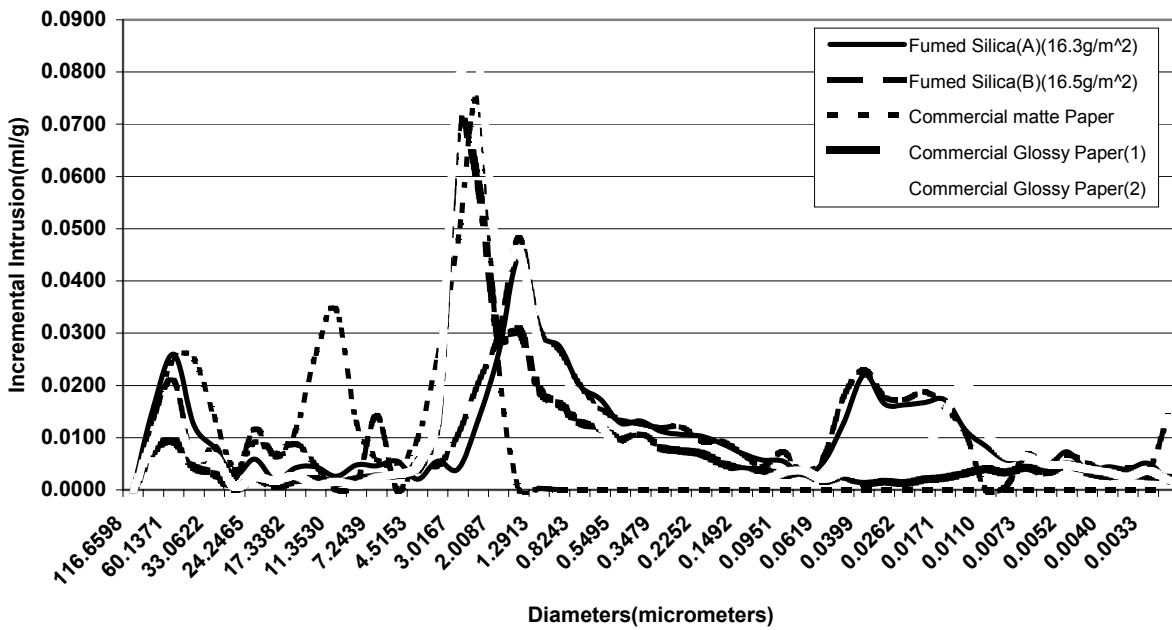


Figure 27. Pore Size Distribution of Fumed Silicas and Commercial Papers by Mercury Intrusion Porosimeter